Cerebral Cortex September 2013;23:2169–2178
doi:10.1093/cercor/bhs192
Advance Access publication August 8, 2012

Feature-Based Attention Affects Direction-Selective fMRI Adaptation in hMT+

Sarah Weigelt[1,2,3], Wolf Singer[1,2,4,5] and Axel Kohler[1,2,6]

[1]Department of Neurophysiology, Max Planck Institute for Brain Research, Frankfurt am Main D-60528, Germany [2]Brain Imaging Center Frankfurt, Frankfurt am Main D-60528, Germany [3]Department of Brain and Cognitive Sciences and McGovern Institute for Brain Research, Massachusetts Institute of Technology, Cambridge, MA 02139, USA [4]Ernst Strüngmann Institute (ESI) for Neuroscience in Cooperation with Max Planck Society, Frankfurt am Main D-60528, Germany [5]Frankfurt Institute for Advanced Studies, Goethe University, Frankfurt am Main D-60438, Germany and [6]Department of Psychiatric Neurophysiology, University Hospital of Psychiatry, University of Bern, Bern 60 3000, Switzerland

Address correspondence to Dr Sarah Weigelt, Massachusetts Institute of Technology, Department of Brain and Cognitive Sciences, McGovern Institute for Brain Research, 77 Massachusetts Avenue, Room 46-4141, Cambridge, MA 02139, USA. Email: weigelt@mit.edu

Functional magnetic resonance adaptation has been successfully used to reveal direction-selective responses in the human motion complex (hMT+). Here, we aimed at further investigating direction-selective as well as position-selective responses of hMT+ by looking at how these responses are affected by feature-based attention. We varied motion direction and position of 2 consecutive random-dot stimuli. Participants had to either attend to the direction or the position of the stimuli in separate runs. We show that direction selectivity in hMT+ as measured by functional magnetic resonance imaging (fMRI) adaptation was strongly influenced by task set. Attending to the motion direction of the stimuli lead to stronger direction-selective fMRI adaptation than attending to their position. Position selectivity, on the other hand, was largely unaffected by attentional focus. Interestingly, the change in the direction-selective adaptation profile across tasks could not be explained by inheritance from earlier areas. The response pattern in the early retinotopic cortex was stable across conditions. In conclusion, our results provide further evidence for the flexible coding of direction information in hMT+ depending on task demands.

Keywords: direction selectivity, motion perception, neuroimaging, repetition suppression, V1

Introduction

To adequately react to a moving object, our visual motion system has to determine several features of that object: Its position in 3D space, its motion direction, as well as its speed. In the present paper, we investigate the effects of feature-based attention—attending to the position of a moving object versus attending to its motion direction—on position- and direction-selective responses in the human motion complex (hMT+).

hMT+ has been identified as a core region for the processing of motion information (Zeki et al. 1991; Watson et al. 1993; Tootell, Reppas, Kwong et al. 1995). Responses in hMT+ and homologous regions in other primates are modulated by feature-based attention as well as task set (Corbetta et al. 1990; 1991; Beauchamp et al. 1997; Chawla et al. 1999; Treue and Martinez-Trujillo 1999; Huk and Heeger 2000; Saenz et al. 2003; Maunsell and Treue 2006; Liu et al. 2007). Furthermore, the amount of attentional modulation depends on the attended feature: hMT+ is more strongly activated when attention is directed toward speed in comparison to color (Corbetta et al. 1990, 1991; Beauchamp et al. 1997; Chawla et al. 1999), shape (Corbetta et al. 1990, 1991), or contrast of a moving object (Huk and Heeger 2000).

First evidence for the direction selectivity of hMT+ in humans came from studies on the motion aftereffect (Tootell, Reppas, Dale et al. 1995; He et al. 1998; Culham et al. 1999; but see Huk et al. 2001). Experiments using functional magnetic resonance imaging (fMRI) adaptation (Huk et al. 2001; Nishida et al. 2003; Ashida et al. 2007; Smith and Wall 2008; Lee and Lee 2012) and employing multivariate pattern analyses (Kamitani and Tong 2006; Serences and Boynton 2007) confirmed and strengthened the finding of direction selectivity in hMT+. With respect to position-selective information, hMT+ presumably contains several retinotopic representations of the contralateral hemifield (Huk et al. 2002; Gardner et al. 2008; Amano et al. 2009; Kolster et al. 2010) with large receptive fields compared with early visual areas (Amano et al. 2009). It is also sensitive to depth (Neri et al. 2004; Brouwer et al. 2005; Likova and Tyler 2007; Smith and Wall 2008; Rokers et al. 2009), thus providing information with regard to the position of a moving object in 3D space.

In the present study, we aimed at extending previous findings by examining not only the effect of feature-based attention on the overall activity of hMT+, but by its effect on selectivity. Using fMRI adaptation, we investigated the response profile of hMT+ during 2 different tasks focusing the observers on changes in motion direction and position, respectively. We were interested in the influence of attentional set on position- and direction-selective adaptation effects. To control whether the effects are inherited from areas lower in the processing hierarchy, we also analyzed the responses in the early retinotopic cortex.

Materials and Methods

Subjects

Twenty-one healthy subjects participated in this study. Subjects were students recruited from the Goethe University of Frankfurt or members of the Frankfurt neuroscience community and gave their informed written consent to the procedure in accordance with institutional guidelines and the Declaration of Helsinki. All subjects had normal or corrected-to-normal vision and were right-handed as assessed by an adapted version of the Edinburgh Handedness Scale. The data from one subject had to be excluded because of excessive head motion. From the remaining 20 subjects (9 female; mean age: 24.85 years; range: 20–32 years), 5 additional subjects had to be excluded during data analyses because of their low behavioral performance (<70% correct responses) in the direction task (see below). Of the remaining 15 subjects, 6 were female, the mean age was 25.4 years and the age range was 20–32 years. The study was approved by the ethics committee of the Medical School of the University Clinics Frankfurt.

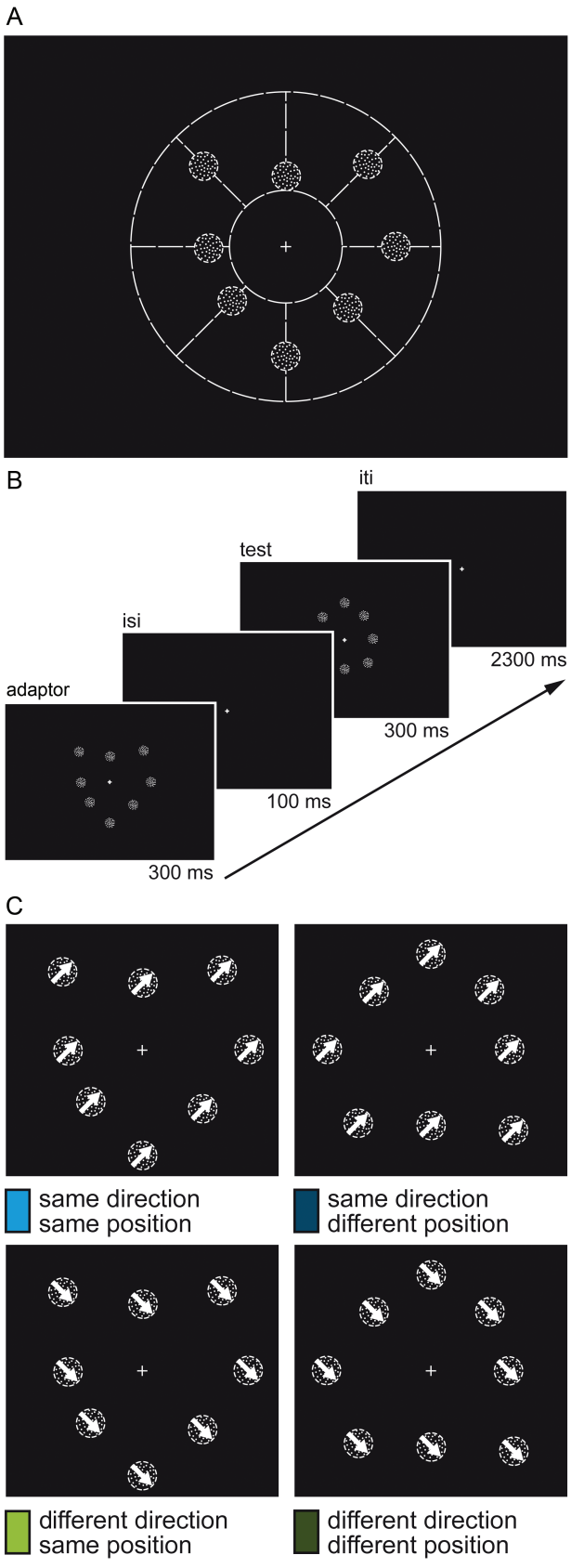

Figure 1. Stimulus and experimental design. (*A*) Scaled illustration of the stimulus. The stimulus consisted of 8 circular random-dot apertures (each sized 1.5° visual angle) that contained 40 moving white dots (each 0.056° visual angle) on a black background. The random-dot apertures were aligned onto radii whose central point was in the middle of the screen. The position of each random-dot aperture on its radius was chosen randomly for each trial, but restricted to an annulus between 3° and 8.25° visual angle. (*B*) Sequence of an experimental trial. Each trial started with the presentation of the adaptor stimulus (adaptor) for 300 ms, followed by a blank interstimulus interval for 100 ms. Then, the test stimulus (test, in this case showing a position change) was presented for 300 ms. The trial ended with a 2300 ms intertrial interval, in which subjects responded according to the task. Adaptor and test were movies of white dots within random-dot apertures. Throughout the visual stimulation, a fixation cross was shown at the center of the screen. (*C*) Schematic illustration of the 4 different experimental conditions. The test was varied along the dimensions "position of the random-dot apertures" (same/different) and "motion direction of the dots" (same/different) with regards to the adaptor. This led to 4 experimental conditions: A test that was identical to the adaptor (same direction–same position, cyan), a test in which the position changed, but the motion direction was the same (same direction–different position, dark blue), a test in which the motion direction changed, but the position of the random-dot apertures remained the same (different direction–same position, light green), or a test in which both the motion direction and the position changed (different direction–different position, dark green). Dotted white circles and lines, as well as white arrows, were not actually shown but aid visualization.

Procedure

Scanning took place at the Brain Imaging Center, Frankfurt, Germany. All subjects were measured on 2 separate days: Once for the adaptation experiment (both tasks) and once for the mapping experiment. The mapping session was always after the adaptation experiment, separated by approximately 8 weeks.

Apparatus

Visual stimuli were delivered via a video goggle system (VisuaStim Digital Glasses; Resonance Technology, Northridge, CA, United States of America). The refresh rate of the goggle monitors was set to 60 Hz for all stimuli. A custom-made fiber-optic button box allowed the subjects to communicate their decisions in the behavioral tasks.

Adaptation Experiment

Stimuli

Visual stimuli were programmed using custom-made C++ code. The stimulus consisted of 8 circular apertures (random-dot aperture; with a size of 1.5° visual angle) that contained 40 moving white dots (each 0.056° visual angle) on a black background (Fig. 1*A*). The random-dot apertures were aligned onto radii whose central point was in the middle of the screen. The position of each random-dot aperture on its particular radius was chosen randomly for each experimental trial, but restricted to an annulus between 3 and 8.25° visual angle. The dots of all random-dot apertures moved with 100% coherence (unlimited lifetime) and a speed of 6.78° visual angle per second on one of the diagonals (45°, 135°, 225°, or 315°). It is important to emphasize that the dots within the apertures moved, but the apertures themselves remained stationary. One stimulus consisted of 300 ms of a random-dot sequence, presented at a frame rate of 60 Hz. A white fixation cross (sized 0.57 × 0.57° visual angle) was always displayed in the middle of the screen.

Experimental Design

Figure 1*B* displays the course of an experimental trial that began with the presentation of the adaptor stimulus for 300 ms followed by a blank interstimulus interval (only the fixation cross was present) lasting 100 ms. Then, the test was presented for 300 ms. After that, a blank screen was displayed for 2300 ms, yielding a trial duration of 3000 ms in total. Figure 1*C* displays the different experimental conditions defined by variations of the test. The test could be a repetition of the adaptor in terms of the motion direction of the dots and the position of the random-dot apertures ("same direction–same position"), or varied from the adaptor either with respect to the position of the apertures ("same direction–different position") or with respect to the motion direction of the dots ("different direction–same position") or with respect to both the position of the apertures and the motion direction of the dots ("different direction–different position").

The first and last experimental conditions served as lower and upper boundaries for the expected adaptation effects.

A change in the position of the random-dot apertures was defined by a shift of each aperture along their respective radii either toward or away from the center of the screen (fixation cross). The shift subtended 3.23° visual angle from center to center of the aperture, thus creating a gap of 0.23° visual angle between the old and the new outer border of the aperture. The inward/outward shift of all apertures together was set such that the average eccentricity of the adaptor and the test stimulus remained the same. A change in the motion direction of the dots was defined by a +90° or −90° step.

The order of the presentation of the experimental trials was counterbalanced across runs per subject (i.e. trials from each condition [fixation included] were preceded [two trials back] equally often by trials from each other condition). Because of this strategy, the first 3 experimental trials (which had no adequate history) were excluded from the analyses.

For the adaptation experiment, subjects underwent 6 experimental runs (7 min each; 3 runs per behavioral task) and an anatomical run (9 min 38 s). Each experimental run began with a fixation point presented for 16 s, then followed by an experimental block consisting of 125 trials, 3 s each (100 experimental trials, plus 25 fixation trials, plus 3 extra trials; see below). At the end of each run, a fixation point was shown for 16 s. In summary, each experimental run had 25 trials per experimental condition, resulting in 75 trials per subject per experimental condition for each of the 2 behavioral tasks.

Behavioral Task

Subjects were instructed to maintain fixation on the center cross throughout the experimental run, while performing the behavioral tasks. The behavioral task always consisted in a same/different comparison between the test and the adaptor. In one half of the experimental runs, subjects were asked to indicate via a button press whether the random-dot apertures were at the same positions in the test as in the adaptor or whether their positions had changed ("attention-to-position task"). In the other half of experimental runs, subjects had to indicate via a button press whether the motion direction of the dots was the same in the test as in the adaptor or whether the motion direction had changed ("attention-to-direction task"). Subjects did not receive feedback on their performance.

Subjects performed 3 runs of each task, which were separated by the anatomical run, for example, they started with 3 runs performing the attention-to-position task, then followed the anatomical run, and then they continued with 3 runs now performing the attention-to-direction task or vice versa. The order of tasks was counterbalanced across subjects. Subjects always responded with their right index and middle finger—the association of same/different to the 2 fingers was counterbalanced across subjects.

We analyzed percent correct responses and median reaction times. We chose to analyze median reaction times instead of mean reaction times because we did not explicitly instruct our subjects to respond as fast as possible and therefore were aiming at a stable measure of reaction time. Responses were defined by a button press in an interval between 500 and 2000 ms after the onset of the adaptor (which equals 100 and 1600 ms after the onset of the test). If no button press was detected in that time window, this was counted as a miss. Also, only the first button press was taken into account; if a second button press occurred, this was ignored. Data were averaged across runs (3 runs per task) per subject. The mean percent correct was 84.35% for the attention-to-direction task (standard deviation [SD], 10.89) and 96.86% (SD, 2.80) for the attention-to-position task. Ranking the subjects according to their performance in the attention-to-direction task and contrasting this performance with the performance in the attention-to-position task, we found that the performance of 5 subjects was below 1 SD of the average with <70% correct responses in the attention-to-direction task (while performance in the attention-to-position task was similar across subjects) and thus excluded those subjects from further analyses. Note that this procedure did not lead to a complete matching of task difficulty. The remaining 15 subjects performed above 85% correct in both tasks

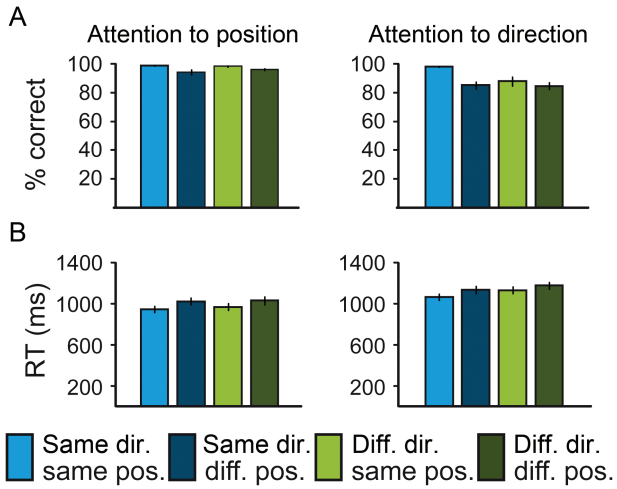

Figure 2. Behavioral results. Bar plots show percent correct responses (*A*) and median reaction times (*B*) averaged across participants for the 4 experimental conditions and the 2 tasks separately.

(Fig. 2), with 89.28% (SD, 6.48) in the attention-to-direction task and 97.12% (SD, 2.47) in the attention-to-position task. The attention-to-direction task was significantly more difficult than the attention-to-attention task (paired *t*-test, $t(14) = 4.66$, $P < 0.001$). However, a full difficulty matching was impossible to achieve, as it would have meant either decreasing the saliency of the position change or increasing the saliency of the direction change. Decreasing the position change was not possible, as it would have resulted in an overlap of the two apertures in the different condition, which in turn would have abolished the rebound effect to a change in position and participants' performance was already at ceiling. Increasing the direction change was not possible either: In pilot experiments, we tried various speeds and also a change in direction of 180° instead of 90°–none led to a higher performance in the task. Thus, a complete matching of task difficulty was impossible for the intended design and research question. Importantly, however, we restricted our fMRI analyses to correct trials only. For a full analysis of the behavioral data, we computed repeated-measures ANOVAs with the factors "direction" (same and different) and "position" (same and different), separately for each task on percent correct responses (Fig. 2*A*) and median reaction times (Fig. 2*B*). With regard to percent correct responses, both tasks reveal a main effect for the position. The attention-to-direction task furthermore shows a main effect for the direction. With regard to median reaction times, all main effects and the interactions were significant (Supplementary Table 1).

fMRI Data Acquisition

Blood oxygenation level-dependent (BOLD) fMRI was performed on a 3 T Siemens Allegra scanner (Siemens, Erlangen, Germany) equipped with a 4-channel head coil at the Brain Imaging Center, Frankfurt am Main, Germany.

Adaptation Experiment

A gradient-recalled echo-planar imaging sequence was used with the following parameters: Number of slices, 20; repetition time (TR), 1000 ms; echo time (TE), 25 ms; slice thickness, 4.5 mm; in-plane resolution, 3.3×3.3 mm^2; gap thickness, 0.45 mm. The slices were oriented to reach a total coverage of the occipital and parietal lobes and usually most of frontal and temporal lobes. In case a full coverage of the brain was not achievable, the orbitofrontal cortex and anterior portions of the temporal lobes were not covered. Functional images were acquired in 6 experimental runs in a single session. Each run comprised the acquisition of 420 volumes. Stimulus presentation was synchronized with the fMRI sequence at the beginning of each run.

Each scanning session included the acquisition of a high-resolution magnetization-prepared rapid-acquisition gradient echo sequence for coregistration and anatomical localization of functional data (TR, 2250 ms; TE, 4.38 ms; voxel size, $1 \times 1 \times 1$ mm^3).

Mapping Experiment

For the mapping experiment, slightly different sequence parameters were used: Number of slices, 40; TR, 2000 ms; TE, 25 ms, slice thickness, 3 mm; in-plane resolution, 3×3 mm^2; gap thickness, 0.3 mm. With these parameters, we achieved whole-brain coverage.

fMRI Data Preprocessing

Data analysis and visualization was performed using the BrainVoyager QX software package (Version 1.10.3; Brain Innovation, Maastricht, The Netherlands). We first evaluated raw fMRI data quality in terms of technical artifacts such as signal jumps. We detected signal jumps that were caused by a temporarily malfunctioning head coil in 4 runs (1 run from the position task and 3 runs from the direction task; out of a total of 90 runs), and excluded these runs from further analyses. The first 4 volumes of each event-related run were discarded to preclude T1-saturation effects. Preprocessing of the functional data included 1) 3D motion correction, 2) linear trend removal and temporal high-pass filtering at 0.01 Hz, and 3) slice scan-time correction with sinc interpolation. We also employed a spatial smoothing of 6 mm full-width at half-maximum. For each subject, the functional and structural 3D data sets were transformed into Talairach coordinate space (Talairach and Tournoux 1988). The recorded high-resolution anatomies of all subjects were used for surface reconstruction, which included gray/white-matter segmentation based on intensity values. The cortical surfaces were slightly smoothed and inflated.

Our rapid event-related fMRI study used closely spaced trials, leading to a substantial overlap in the resulting hemodynamic responses. Nevertheless, under the assumption of linearity, the underlying hemodynamic responses can be assessed by deconvolution (Dale and Buckner 1997). A deconvolution analysis estimates the hemodynamic response function for each trial on the basis of a general linear model (GLM). Twenty predictors were defined to cover the temporal extent of a typical hemodynamic response. Because of the hemodynamic lag in the BOLD response, differences between conditions (as well as the peak in overall response) are expected to occur at a lag of several seconds after stimulus onset (Boynton et al. 1996; Cohen 1997). On the basis of the deconvolved fMRI signal, we identified the peak points at lags 4 and 5 s after trial onset.

Mapping Experiment: Definition of Regions of Interest

hMT+

We mapped hMT+ in each subject individually with a design containing blocks of full-field stimulation with a coherent flowfield stimulus, an incoherent flowfield stimulus, a flickering stimulus, a static stimulus, and pure fixation. During the mapping experiment, subjects were instructed to fixate thoroughly on the fixation cross, which was visible at all times at the center of the screen. No additional behavioral task was employed. We acquired one functional run lasting 9 min 4 s.

hMT+ was defined by contrasting the blocks with a coherent flowfield stimulus to blocks with a static stimulus. The known Talairach coordinates and anatomical landmarks were used as additional constraints. Statistical thresholds were adjusted for each subject individually to yield a size of the regions of interest (ROIs) of approximately 400 voxels (voxel size: $1 \times 1 \times 1$ mm^3) per hemisphere. Usually, thresholds were set at $P < 0.001$. In 3 subjects, thresholds had to be lowered to achieve sufficient voxel numbers (Subject 3: $P = 0.015$, Subject 6: $P = 0.046$, and Subject 13: $P = 0.002$). However, in Subject 6 even at this low threshold, the hMT+ ROI in the right hemisphere subtended only 300 voxels (instead of the intended 400). Table 1 provides an overview of *t*-/*P*-values for the individual thresholds as well as the number of voxels and Talairach coordinates for all hMT+ ROIs. Figure 3*A* shows hMT+ ROIs of all subjects.

Visual Areas V1, V2, V3, hV4, and V3A/B

Mapping of retinotopic visual areas consisted of a polar-angle mapping as has been described in detail elsewhere (Muckli et al. 2006). In brief, we presented a black-and-white checkerboard pattern that consisted of a wedge-shaped disk segment subtending 22.5° of polar angle. The aspect ratio of the checks was kept constant by scaling their height linearly with eccentricity. The wedge started at the right horizontal meridian and slowly rotated clockwise for a full circle of 360° within 96 s. Subjects were instructed to fixate on the center. The mapping included 10 full cycles of the rotating wedge. One functional run lasted 13 min 16 s.

Cross-correlation analyses were performed and the resulting phase-encoded maps were projected onto the cortical hemispheres of the individual subjects. We manually drew borders between visual areas along vertical and horizontal meridians. Areas were shaded in light gray. The border definition of V1, V2, and V3 is currently not under debate. In the more disputed case of hV4 and V3A/B, we followed the criteria of Wandell et al. (2007). We were unsure about the border separating V3A from V3B, and since Smith and Wall (2008) showed that direction-selective fMRI adaptation in areas V3A and V3B did not differ, we pooled both areas to one area complex V3A/B. We

Table 1
Talairach coordinates, number of voxels, and statistical thresholds for hMT+

Subject	Left hemisphere				Right hemisphere				*t*-value, left (*t*-value, right)	*P*-value, left (*P*-value, right)
	x	*y*	*z*	No. of voxels	*x*	*y*	*z*	No. of voxels		
1	−43	−64	2	404	42	−61	1	406	5.70 (5.70)	<0.001 (<0.001)
2	−44	−65	14	400	51	−62	3	406	5.77 (4.17)	<0.001 (<0.001)
3	−40	−66	7	403	40	−55	1	398	2.46 (2.46)	0.015 (0.15)
4	−47	−65	5	406	36	−62	−2	403	5.90 (4.90)	<0.001 (<0.001)
5	−43	−74	7	392	44	−66	1	395	5.40 (5.40)	<0.001 (<0.001)
6	−46	−67	4	406	43	−68	2	300	2.00 (2.00)	0.046 (0.046)
7	−43	−68	14	400	39	−59	2	400	3.80 (3.80)	<0.001 (<0.001)
8	−43	−72	6	404	43	−67	8	406	6.90 (6.90)	<0.001 (<0.001)
9	−45	−65	6	400	39	−64	1	399	4.80 (3.40)	<0.001 (<0.001)
10	−45	−67	0	404	47	−59	3	397	4.40 (4.15)	<0.001 (<0.001)
11	−48	−70	2	407	48	−62	5	414	3.65 (3.65)	<0.001 (<0.001)
12	−40	−62	5	395	39	−52	1	391	7.57 (7.57)	<0.001 (<0.001)
13	−45	−72	8	388	50	−60	5	409	3.10 (3.10)	0.002 (0.002)
14	−48	−65	3	395	42	−60	6	404	3.70 (3.70)	<0.001 (<0.001)
15	−46	−72	4	397	49	−63	0	398	7.42 (7.42)	<0.001 (<0.001)
Mean	−44	−68	6	400	43	−61	2	395		
SD	2	4	4	6	5	4	3	27		

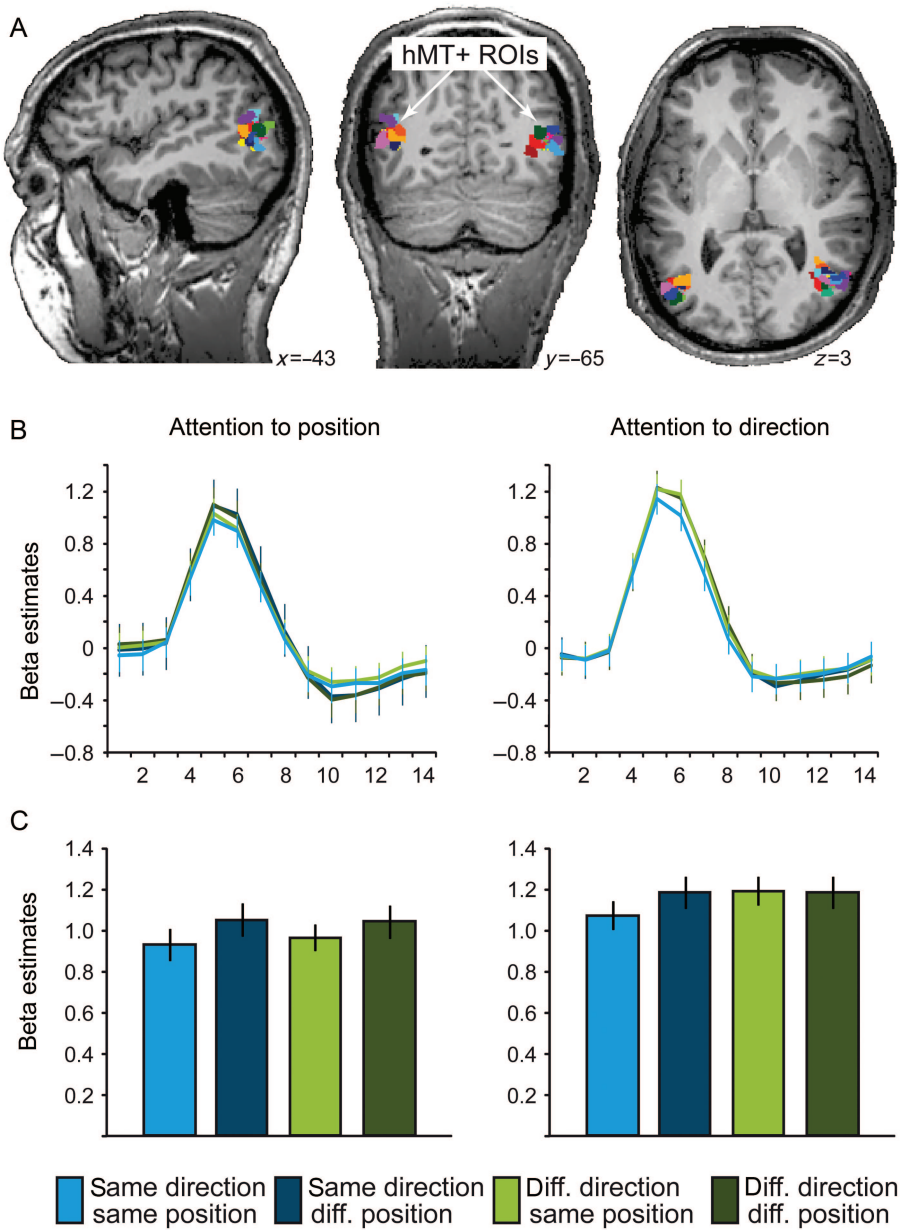

Figure 3. hMT+ results. (*A*) Individual hMT+ ROIs of 15 subjects (every color indicates a different subject) displayed on 3 anatomical slices of 1 representative subject. Coordinates indicate Talairach coordinates. (*B*) Beta estimates (event-related deconvolved BOLD-signal time course) from hMT+ ROIs averaged across trials and subjects for each of the 2 tasks. Time point 1 corresponds to stimulation onset. (*C*) Beta estimates (average of peak points 4 and 5 of the event-related deconvolved BOLD response) from hMT+ ROIs averaged across trials and subjects for each of the 2 tasks. Error bars indicate ± SEM across subjects; df = 14; diff., different.

identified V1, V2, V3 (dorsal and ventral subparts), and V3A/B in 15 out of 15 subjects. hV4 was identified reliably in 11 out of 15 subjects.

To render ROIs in visual areas V1, V2, V3, hV4, and V3A/B more precisely, we used an activation map based on the adaptation experiment in conjunction with the retinotopic map in each subject and hemisphere. We computed for each subject a GLM for the adaptation experiment across all experimental runs (and thus across behavioral tasks) and contrasted (at peak points 4 and 5 s after adaptor onset) all experimental conditions against the baseline to display a map of general activation in relation to the visual stimulation. We thresholded the activation map at $P < 0.05$ (Bonferroni corrected). We projected the activation map onto the reconstructed cortical surfaces, superimposing the predefined retinotopic map (Fig. 4*A*). ROIs were defined at the overlay of the activation map and the retinotopic map. We chose to place the ROIs in middle eccentricity, as this was the eccentricity stimulated most reliably in all our participants. We did not have any a priori hypothesis regarding differences in fMRI adaptation effects depending on eccentricity and thus did not test other eccentricities. Furthermore, as can be seen from the whole-brain analysis (Supplementary Fig. 1), position-selective fMRI adaptation was indeed distributed across all eccentricities covered by our annulus stimulus. For each subregion (dorsal and ventral) of V1, V2, and V3 ROIs encompassed 200 voxels per hemisphere, and for areas hV4 and V3A/B 400 voxels to reach a size of 400 voxels on average per hemisphere of each and every ROI defined in this study (including hMT+, see above).

We compared the number of voxels for all ROIs (V1, V2, V3, hV4, and hMT+) and found that they did not differ between visual areas (repeated-measures ANOVA with single factor "visual area" at 6 levels [V1, V2, V3, hV4, V3A/B, and hMT+], $F_{5,10} = 1.812$, $P = 0.198$).

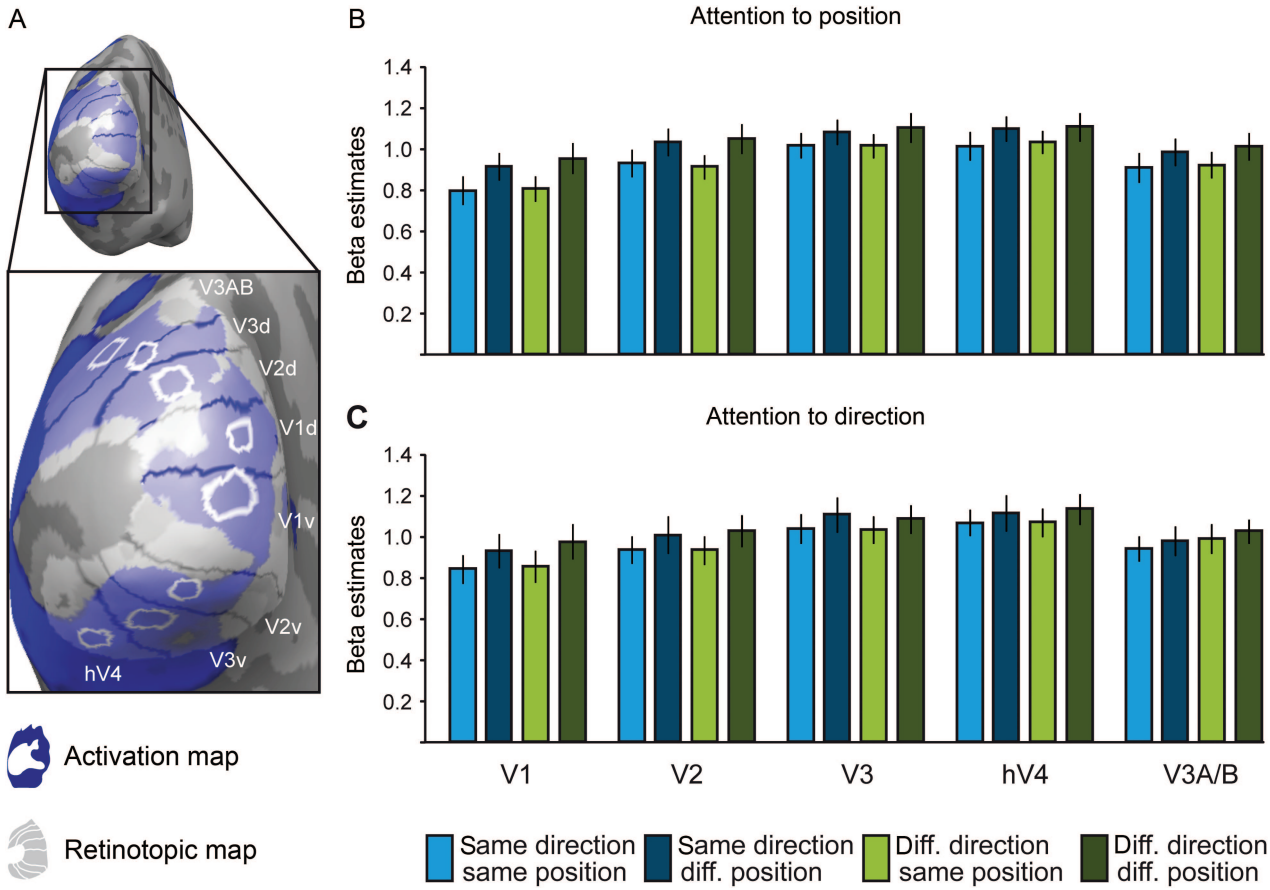

Figure 4. Results for visual areas V1, V2, V3, hV4, and V3A/B. (*A*) Full picture and close-up of a reconstructed and inflated left cortical hemisphere of one representative subject, viewed from the back (with a focus on the occipital pole). The individual retinotopic map derived from standard polar angle mapping procedures (shown in gray) and an individual activation map (shown in blue) are superimposed. White circles mark the defined ROIs. (*B* and *C*) Beta estimates (average of peak points 4 and 5 of the event-related deconvolved BOLD fMRI response) for the different ROIs in the visual cortex (V1, V2, V3, hV4, and V3A/B), separately for the attention-to-position task (*B*) and for the attention-to-direction task (*C*). Peak averages are averaged across trials and subjects. Error bars indicate ± SEM across subjects; df = 14; d, dorsal; diff., different; v, ventral.

Statistical Analysis

For the ROI analyses, we extracted the deconvolved time course averaged across runs, separately for the 2 tasks, of each subject from their individual ROIs. Per subject, we thus obtained for each ROI an estimate of the BOLD signal for each experimental condition at 20 time points (in steps of 1 s) following stimulation onset. The fully deconvolved time course of hMT+ averaged across subjects can be seen in Figure 3*B*. Via visual inspection, we identified time points 4 and 5 as the peak points. For the statistical analyses, we focused only on the peak points. We averaged the 2 peak points per experimental condition and ROI and subject. We did not find any differences between subregions (dorsal and ventral) nor hemispheres for any of the ROIs and thus averaged across subregions and hemispheres. We ended up with one beta weight per experimental condition and ROI and subject and used these data as input to our second-level statistics. Statistics were performed with SPSS (version 12.0.1, SPSS Inc., Chicago, IL, United States of America). We computed 2-way multivariate ANOVAs for the 2 tasks separately with factors "direction" (same, different) and "position" (same, different) for all ROIs (V1, V2, V3, hV4, V3A/B, and hMT+).

Results

We manipulated feature-based attention by instructing subjects to perform 2 different behavioral tasks on the same stimulus material. Briefly, our stimulus contained 8 random-dot apertures with white dots on a black background (Fig. 1*A*). Two short movie sequences (first the adaptor movie then the test movie) of the dots within their apertures where shown, separated by a very short interval (Fig. 1*B*). Different experimental conditions were created by varying the test stimulus (Fig. 1*C*): The test could be a repetition of the adaptor in terms of the motion direction of the dots and the position of the random-dot apertures (same direction–same position), or varied from the adaptor either with respect to the position of the apertures (same direction–different position) or with respect to the motion direction of the dots (different direction–same position) or with respect to both position of the apertures and motion direction of the dots (different direction–different position). To manipulate feature-based attention, we had subjects perform 2 different behavioral tasks: In half of the experimental runs, subjects were instructed to report whether the test stimulus moved in the same direction as the adaptor stimulus (attention-to-direction task), while in the other half of the experimental runs, subjects had to report whether the apertures of the test stimulus were at the same position as the apertures of the adaptor stimulus (attention-to-position task).

fMRI Results

For the analyses of fMRI data, we only included correct trials. The main focus of our study was the analysis of ROIs, hMT+ as well as early visual areas V1, V2, V3, hV4, and V3A/B.

hMT+

We defined hMT+ in each subject individually in both hemispheres based on a separate localizer experiment (Fig. 3*A*). Table 1 provides the numbers of voxels for each ROI, as well as Talairach coordinates and statistical thresholds at which ROIs were defined (see the Materials and Methods section for a more detailed description of the procedure). For the main experiment, we then extracted fMRI signals from each subject's hMT+ and used them for second-level statistics. Because we did not observe differences in response patterns between left and right hMT+, we pooled data from the 2 hemispheres and performed 2-factorial ANOVAs ("position" [same, different] × "direction" [same, different]) for the 2 tasks. In the attention-to-position task, hMT+ displayed a significant position-selective fMRI adaptation (Fig. 3*B* and *C*; main effect "position," $F_{1,14} = 10.45$, $P = 0.006$, $\eta^2 = 0.43$) and no other effects ($P > 0.37$). In the attention-to-direction task, the main effect for "position" was preserved ($F_{1,14} = 4.97$, $P = 0.04$, $\eta^2 = 0.26$), but most interestingly now there was also a main effect for direction ($F_{1,14} = 6.06$, $P = 0.03$, $\eta^2 = 0.30$) and the interaction "position" × "direction" reached significance ($F_{1,14} = 4.97$, $P < 0.05$, $\eta^2 = 0.25$). As can be seen in Figures 3*B* and *C*, these differences between tasks arise through a task-specific rebound from adaptation for the condition "same position–different direction" compared with "same position–same direction" (attention-to-position task: $t(14) = -1.02$, $P = 0.33$; attention-to-direction task: $t(14) = -3.33$, $P = 0.005$).

Visual Areas V1, V2, V3, hV4, and V3A/B

We defined ROIs for visual areas V1, V2, V3, hV4, and V3A/B for each subject based on individual retinotopic mapping and activation maps (Fig. 4*A*; see the Materials and Methods section). Again, fMRI signals were extracted from these regions from each subject and used for second-level testing. In the attention-to-position task, all visual areas showed position-selective fMRI adaptation (Fig. 4*B*; main effect "position", V1: $F_{1,14} = 32.24$, $P < 0.001$, $\eta^2 = 0.70$; V2: $F_{1,14} = 41.56$, $P < 0.001$, $\eta^2 = 0.75$; V3: $F_{1,14} = 29.37$, $P < 0.001$, $\eta^2 = 0.68$; hV4: $F_{1,14} = 17.69$, $P = 0.001$, $\eta^2 = 0.56$; V3A/B: $F_{1,14} = 21.92$, $P < 0.001$, $\eta^2 = 0.61$) and no main effect for "direction" and no interaction effect ($P > 0.28$). In the attention-to-direction task, the main effect "position" was weakened in all areas and remained significant only for V1 and V2 (Fig. 4*C*; main effect "position", V1: $F_{1,14} = 13.68$, $P = 0.002$, $\eta^2 = 0.49$; V2: $F_{1,14} = 5.18$, $P = 0.04$, $\eta^2 = 0.27$; other areas: $P > 0.08$). Again, no other effects were significant ($P > 0.18$).

Overall Attention Effect

To assess the overall influence of the task on the BOLD signal level, we computed paired comparisons between tasks for the condition "same position–same direction". This was to avoid the influence of differential adaptation effects in the other conditions that might confound pure attentional effects on the BOLD signal. Only for hMT+, we found a significant increase in the peak response estimate of 14.9% in the attention-to-direction task compared with the attention-to-position task ($t(14) = 2.27$, $P = 0.04$). The responses in all other areas were unaffected by task set (difference <5.5%, $P > 0.28$).

Whole-Brain Analyses

To assess the specificity of our hypothesis-driven ROI-based analyses, we performed complementary whole-brain analyses (Supplementary Fig. 1). Supporting our ROI-based analyses, task-specific activations as reported in the section "Overall attention effect" were found mainly in hMT+. Furthermore, position-specific adaptation effects were widely distributed in the visual cortex as expected since position-specific adaptation effects in a whole-brain analysis is another way of identifying retinotopic areas. Analogous to our ROI analysis, position specificity was reduced in the attention-to-direction task in comparison to the attention-to-position task. Direction-selective adaptation effects were revealed in one region in the parietal cortex anterior and ventral to V3A/B. Importantly, no prominent regions were revealed showing a similar profile as the one of hMT+ in our ROI-based analyses, suggesting that the adaptation profile of hMT+ in our task set is not likely driven by top-down effects as, for example, shown in the ventral visual pathway (Ewbank et al. 2011). This might be because of the nature of our fast event-related adaptation paradigm with intermixed experimental conditions.

Notes on Eye Movements

It is conceivable that the 2 tasks evoked different eye movements, which would have influenced our fMRI results. We think this is unlikely for 3 reasons: 1) Even if the number of eye movements or their duration would be different between the 2 tasks, we would not expect such distinct response profiles for hMT+ in comparison to V1 or between the 2 tasks for hMT+; 2) unstable fixation would have resulted in a loss of position-selective adaptation; and 3) the position of the random-dot apertures was randomly set at the beginning of each experimental trial as was the motion direction and position change. Thus, it was impossible for the subjects to make a predictive saccade. Other aspects of our stimulus further aided fixation: The presence of a fixation cross throughout the complete run and the fact that in trials, in which the position changed, these changes were set for each random-dot aperture randomly to be either toward or away from the fixation, thereby not creating a coherent motion percept.

Discussion

The present study investigated the modulation of fMRI adaptation effects in hMT+ by 2 attention tasks focusing on different aspects of the stimulus, direction, and position. Although in both tasks attention was directed toward the stimulus, the adaptation profile in hMT+ changed. Whereas position effects were largely unaffected by the task, signal rebounds for direction changes were only detectable in the attention-to-direction task. This pattern was specific to hMT+ when compared with early visual areas. In addition, only in hMT+, the overall signal level (magnitude of beta weights) was higher for the attention-to-direction task relative to the attention-to-position task, indicating a regionally selective gain increase.

The Impact of Feature-Based Attention on fMRI Adaptation

A characteristic feature of our study is that we investigated the influence of feature-based attention not on fMRI responses per se, but on fMRI adaptation effects, thereby revealing modulations of population selectivity not described before. In early visual areas, fMRI adaptation does not seem to be strongly affected by feature-based attention: Murray et al. (2006) investigated position-selective adaptation in V1, V2,

and V3, while subjects were either performing a same/different task on the position of the stimulus or a change-in-luminance detection task on the fixation center. Position-selective adaptation effects did not differ between these 2 tasks. Furthermore, adaptation effects in early visual areas are also not strongly influenced by attentional mechanisms in general: They can be enhanced if the attentional focus is on the adapting feature (Liu et al. 2007), but they can also be detected when attention is drawn away from the adapting feature to the center of the screen (Larsson et al. 2006; Murray et al. 2006).

fMRI adaptation in higher-level visual areas, however, is strongly influenced by attention. Spatial attention (Eger et al. 2004; Murray and Wojciulik 2004; Henson and Mouchlianitis 2007) and object-based attention (Vuilleumier et al. 2005; Yi and Chun 2005; Yi et al. 2006) significantly enhance adaptation effects, and sometimes only attended objects seem to elicit adaptation effects at all in higher-level areas (Weigelt et al. 2007). Interestingly, however, as long as subjects' attention is focused on the stimuli, the type of behavioral task being performed on the objects (and thus the feature being attended) does not seem to have a strong effect on adaptation in higher-level visual areas. Murray and Wojciulik (2004) contrasted a task in which subjects had to judge if the second object was rotated to the left or the right in comparison to the first object with a task in which they had to judge whether it was the same or a different object. Both tasks evoked similar rotation-selective adaptation effects in the lateral occipital complex. Similarly, fMRI adaptation in the parahippocampal place area occurred for very similar images in comparison to different images, no matter if subjects judged if 2 images were taken from the same overall scene or if the 2 images were identical pixel-by-pixel (Xu et al. 2007).

In contrast to these previous studies, we did find clear changes in the adaptation profile of hMT+, although for both tasks, the attention was directed toward the stimulus. Focusing on the motion direction in contrast to the position reveals a direction-selective rebound in the BOLD response in addition to the position-selective adaptation effect. In other words, direction-selective adaptation effects in hMT+ are contingent on attention being focused on the motion direction—a novel finding. It is unlikely that differences in spatial attention between tasks alone provide an explanation for this pattern. Although the BOLD signal was enhanced in hMT+ for the attention-to-direction compared with the attention-to-position task, a hallmark of spatial attention is a strong modulation of all visual areas, especially with comparable effects in other intermediate-level visual areas, like hV4 and V3A (Tootell et al. 1998; Kastner et al. 1998; Gandhi et al. 1999; Kastner et al. 1999; Somers et al. 1999), which was not the case in our study.

The stronger activation in hMT+ for the attention-to-direction task in comparison to the attention-to-position task is in line with previous research, which has shown that the overall activity level in hMT+ is higher when attention is directed toward a feature that is more relevant to processing in hMT+, such as speed, in contrast to a feature that is less relevant, such as color (Corbetta et al. 1990, 1991; Beauchamp et al. 1997; Chawla et al. 1999). However, such a scaling of responses is not sufficient to explain the major change in adaptation profiles between tasks. Whereas no significant response rebound could be detected for direction changes in the attention-to-position task, the direction-selective rebound reached ceiling in the attention-to-direction task. A qualitatively similar effect has been described in a study using multivoxel pattern analysis by Peelen et al. (2009). They looked for category information present in an object-selective region of the ventral visual pathway. Subjects had to either report the presence of cars ("car task") or people ("body task") in scenes. Multivariate pattern information with regard to cars was present only during the car task, and body information was present only during the body task, independent of spatial attention. Our results suggest that a similar effect occurs for fMRI adaption in hMT+. Only when attention is focused on the motion direction, segregation of neural populations representing orthogonal motion directions leads to a direction-selective signal rebound. Our findings thus argue for a strong effect of attention on direction selectivity in hMT+, at least as measured by fMRI adaptation.

However, our results also show that position-selective fMRI adaptation effects are an exception to the rule that fMRI adaptation effects in higher-level visual areas are strongly affected by attention. Position information was coded in most if not all visual areas even if attention was diverted to another feature of the stimulus lending further support to the notion that the encoding of position information is one of the core organizational principles of most of the visual cortex, particularly early visual areas and regions in the dorsal pathway.

Direction Selectivity in hMT+

By demonstrating direction-selective adaptation in hMT+, we replicate several previous findings (Huk et al. 2001; Nishida et al. 2003; Ashida et al. 2007; Smith and Wall 2008). One difference to these previous studies is that we used a classic event-related adaptation paradigm that did not contain any long adaptation periods, but only brief (300 ms) presentations of stimuli and has been shown to primarily target adaptation responses in extrastriate areas (Weigelt et al. 2008). It is important to note that in our data, the direction-selective fMRI adaptation in hMT+ cannot be easily explained by a mere inheritance from V1. Neither V1 nor any other area receiving direct input from V1 showed direction-selective fMRI adaptation in our study.

Position Selectivity in hMT+

As expected, we found strong adaptation to the retinotopic position in areas V1, V2, V3, hV4, and V3A/B. Murray et al. (2006) found similar position-selective adaptation in V1, V2, and V3—even for position shifts of only 0.5° visual angle. These findings are in line with the receptive-field sizes of neurons in areas V1, V2, and V3, which are estimated to be between 0.5 and 2° visual angle (Yoshor et al. 2007; Dumoulin and Wandell 2008). Less position-selective adaptation in hV4 and V3A/B can be explained based on their bigger receptive-field sizes (5° visual angle, Yoshor et al. 2007).

Interestingly, we also found strong position-selective adaptation in hMT+, despite its relatively large receptive-field sizes (Dumoulin and Wandell 2008; Kolster et al. 2010). Studying motion-selective neuronal adaptation in monkey area MT, Kohn and Movshon (2003) found that adaptation to motion did not transfer between 2 portions of the receptive field of a neuron in MT, thus making it likely that the position-selective signal in MT reflects only input from V1. Priebe and Lisberger (2002) and Priebe et al. (2002), however, did investigate the same question, but found the opposite result: Adaptation did

transfer between 2 portions of the receptive field of a neuron in MT. The discrepant results are likely caused by the use of different adaptation approaches (Kohn and Movshon 2003: Long-term adaptation; Priebe and Lisberger 2002 and Priebe et al. 2002: Short-term adaptation) that might target different adaptation mechanisms (Weigelt et al. 2008). In our case, we used a short-term design that is more similar to the one of Priebe et al. Nevertheless, our effects are more in line with the spatially very specific effects of Kohn and Movshon.

In contrast to being merely inherited from an input region, position information might also be computed in hMT+. Using multivariate pattern analysis, Fischer et al. (2010) found precise location information in hMT+. Compared with early visual areas, the response pattern in hMT+ reflected more the perceived position and less the retinotopic coordinates, suggesting an active process of location representation. Furthermore, in behavioral experiments, Wenderoth and Wiese (2008) found very high position selectivity for the direction aftereffect, which is thought to stem from activity in hMT+.

The strong influence of position information on processing in hMT+ might suggest that hMT+ activity reflects local rather than global motion processing. Specifically, the adaptation effects for the direction and position do not add up in the direction task, saturating at the same level for the separate position and direction effects as well as their combination.

In conclusion, while adaptation effects in early visual areas are either only weakly or not at all modulated by the behavioral task or attention in general, adaptation effects in higher-level visual areas are sensitive to the current attentional focus. With the present study, we demonstrate that this applies not only to spatial, but also to feature-based attention. Interestingly, this effect obtains only for motion direction, a feature for which hMT+ is highly selective, and is not inherited from areas earlier in the processing hierarchy.

Supplementary Material

Supplementary material can be found at: http://www.cercor.oxfordjournals.org/.

Funding

This work was supported by the Max Planck Society and the Federal Ministry of Education and Research in Germany (BMBF 01 GO 0508).

Notes

The authors would like to thank Britni Crocker and Tram Nguyen for help with data acquisition and analyses. We thank Christian Altmann, Christoph Bledowski, Oliver Doehrmann, and Benjamin Rahm for fruitful discussions on this project. *Conflict of Interest*: None declared.

References

Amano K, Wandell BA, Dumoulin SO. 2009. Visual field maps, population receptive field sizes, and visual field coverage in the human MT+ complex. J Neurophysiol. 102:2704–2718.

Ashida H, Lingnau A, Wall MB, Smith AT. 2007. FMRI adaptation reveals separate mechanisms for first-order and second-order motion. J Neurophysiol. 97:1319–1325.

Beauchamp MS, Cox RW, DeYoe EA. 1997. Graded effects of spatial and featural attention on human area MT and associated motion processing areas. J Neurophysiol. 78:516–520.

Boynton GM, Engel SA, Glover GH, Heeger DJ. 1996. Linear systems analysis of functional magnetic resonance imaging in human V1. J Neurosci. 16:4207–4221.

Brouwer GJ, van Ee R, Schwarzbach J. 2005. Activation in visual cortex correlates with the awareness of stereoscopic depth. J Neurosci. 25:10403–10413.

Chawla D, Rees G, Friston KJ. 1999. The physiological basis of attentional modulation in extrastriate visual areas. Nat Neurosci. 2:671–676.

Cohen MS. 1997. Parametric analysis of fMRI data using linear systems methods. Neuroimage. 6:93–103.

Corbetta M, Miezin FM, Dobmeyer S, Shulman GL, Petersen SE. 1990. Attentional modulation of neural processing of shape, color, and velocity in humans. Science. 248:1556–1559.

Corbetta M, Miezin FM, Dobmeyer S, Shulman GL, Petersen SE. 1991. Selective and divided attention during visual discriminations of shape, color, and speed: functional anatomy by positron emission tomography. J Neurosci. 11:2383–2402.

Culham JC, Dukelow SP, Vilis T, Hassard FA, Gati JS, Menon RS, Goodale MA. 1999. Recovery of fMRI activation in motion area MT following storage of the motion aftereffect. J Neurophysiol. 81:388–393.

Dale AM, Buckner RL. 1997. Selective averaging of rapidly presented individual trials using fMRI. Hum Brain Mapp. 5:329–340.

Dumoulin SO, Wandell BA. 2008. Population receptive field estimates in human visual cortex. Neuroimage. 39:647–660.

Eger E, Henson RN, Driver J, Dolan RJ. 2004. BOLD repetition decreases in object-responsive ventral visual areas depend on spatial attention. J Neurophysiol. 92:1241–1247.

Ewbank MP, Lawson RP, Henson RN, Rowe JB, Passamonti L, Calder AJ. 2011. Changes in "top-down" connectivity underlie repetition suppression in the ventral visual pathway. J Neurosci. 31:5635–5642.

Fischer J, Spotswood N, Whitney D. 2010. The emergence of perceived position in the visual system. J Cogn Neurosci. 23:119–136.

Gandhi SP, Heeger DJ, Boynton GM. 1999. Spatial attention affects brain activity in human primary visual cortex. Proc Natl Acad Sci USA. 96:3314–3319.

Gardner JL, Merriam EP, Movshon JA, Heeger DJ. 2008. Maps of visual space in human occipital cortex are retinotopic, not spatiotopic. J Neurosci. 28:3988–3999.

He S, Cohen ER, Hu X. 1998. Close correlation between activity in brain area MT/V5 and the perception of a visual motion aftereffect. Curr Biol. 8:1215–1218.

Henson RN, Mouchlianitis E. 2007. Effect of spatial attention on stimulus-specific haemodynamic repetition effects. Neuroimage. 35:1317–1329.

Huk AC, Dougherty RF, Heeger DJ. 2002. Retinotopy and functional subdivision of human areas MT and MST. J Neurosci. 22:7195–7205.

Huk AC, Heeger DJ. 2000. Task-related modulation of visual cortex. J Neurophysiol. 83:3525–36.

Huk AC, Ress D, Heeger DJ. 2001. Neuronal basis of the motion aftereffect reconsidered. Neuron. 32:161–172.

Kamitani Y, Tong F. 2006. Decoding seen and attended motion directions from activity in the human visual cortex. Curr Biol. 16:1096–1102.

Kastner S, De Weerd P, Desimone R, Ungerleider LG. 1998. Mechanisms of directed attention in the human extrastriate cortex as revealed by functional MRI. Science. 282:108–111.

Kastner S, Pinsk MA, De Weerd P, Desimone R, Ungerleider LG. 1999. Increased activity in human visual cortex during directed attention in the absence of visual stimulation. Neuron. 22:751–761.

Kohn A, Movshon JA. 2003. Neuronal adaptation to visual motion in area MT of the macaque. Neuron. 39:681–691.

Kolster H, Peeters R, Orban GA. 2010. The retinotopic organization of the human middle temporal area MT/V5 and its cortical neighbors. J Neurosci. 30:9801–9820.

Larsson J, Landy MS, Heeger DJ. 2006. Orientation-selective adaptation to first- and second-order patterns in human visual cortex. J Neurophysiol. 95:862–881.

Lee AH, Lee SH. 2012. Hierarchy of direction-tuned motion adaptation in human visual cortex. J Neurophysiol. 107:2163–2184.

Likova LT, Tyler CW. 2007. Stereomotion processing in the human occipital cortex. Neuroimage. 38:293–305.
Liu T, Fuller S, Carrasco M. 2007. Feature-based attention modulates orientation-selective responses in human visual cortex. Neuron. 55:313–323.
Maunsell JH, Treue S. 2006. Feature-based attention in visual cortex. Trends Neurosci. 29:317–322.
Muckli L, Kiess S, Tonhausen N, Singer W, Goebel R, Sireteanu R. 2006. Cerebral correlates of impaired grating perception in individual, psychophysically assessed human amblyopes. Vision Res. 46:506–526.
Murray SO, Olman CA, Kersten D. 2006. Spatially specific FMRI repetition effects in human visual cortex. J Neurophysiol. 95:2439–2445.
Murray SO, Wojciulik E. 2004. Attention increases neural selectivity in the human lateral occipital complex. Nat Neurosci. 7:70–74.
Neri P, Bridge H, Heeger DJ. 2004. Stereoscopic processing of absolute and relative disparity in human visual cortex. J Neurophysiol. 92:1880–1891.
Nishida S, Sasaki Y, Murakami I, Watanabe T, Tootell RB. 2003. Neuroimaging of direction-selective mechanisms for second-order motion. J Neurophysiol. 90:3242–3254.
Peelen MV, Fei-Fei L, Kastner S. 2009. Neural mechanisms of rapid natural scene categorization in human visual cortex. Nature. 460:94–97.
Priebe NJ, Churchland MM, Lisberger SG. 2002. Constraints on the source of short-term motion adaptation in macaque area MT. I. the role of input and intrinsic mechanisms. J Neurophysiol. 88:354–369.
Priebe NJ, Lisberger SG. 2002. Constraints on the source of short-term motion adaptation in macaque area MT. II. Tuning of neural circuit mechanisms. J Neurophysiol. 88:370–382.
Rokers B, Cormack LK, Huk AC. 2009. Disparity- and velocity-based signals for three-dimensional motion perception in human MT+. Nat Neurosci. 12:1050–1055.
Saenz M, Buracas GT, Boynton GM. 2003. Global feature-based attention for motion and color. Vision Res. 43:629–637.
Serences JT, Boynton GM. 2007. The representation of behavioral choice for motion in human visual cortex. J Neurosci. 27:12893–12899.
Smith AT, Wall MB. 2008. Sensitivity of human visual cortical areas to the stereoscopic depth of a moving stimulus. J Vis. 8:1.
Somers DC, Dale AM, Seiffert AE, Tootell RB. 1999. Functional MRI reveals spatially specific attentional modulation in human primary visual cortex. Proc Natl Acad Sci USA. 96:1663–1668.
Talairach J, Tournoux P. 1988. Co-planar stereotaxic atlas of the human brain, 3-dimensional proportional systems: an approach to cerebral imaging. New York: Thieme Medical Publishers.
Tootell RB, Hadjikhani N, Hall EK, Marret S, Vanduffel W, Vaughan JT, Dale AM. 1998. The retinotopy of visual spatial attention. Neuron. 21:1409–1422.
Tootell RB, Reppas JB, Dale AM, Look RB, Sereno MI, Malach R, Brady TJ, Rosen BR. 1995. Visual motion aftereffect in human cortical area MT revealed by functional magnetic resonance imaging. Nature. 375:139–141.
Tootell RB, Reppas JB, Kwong KK, Malach R, Born RT, Brady TJ, Rosen BR, Belliveau JW. 1995. Functional analysis of human MT and related visual cortical areas using magnetic resonance imaging. J Neurosci. 15:3215–3230.
Treue S, Martinez-Trujillo JC. 1999. Feature-based attention influences motion processing gain in macaque visual cortex. Nature. 399: 575–579.
Vuilleumier P, Schwartz S, Duhoux S, Dolan RJ, Driver J. 2005. Selective attention modulates neural substrates of repetition priming and "implicit" visual memory: Suppression and enhancements revealed by FMRI. J Cogn Neurosci. 17:1245–1260.
Wandell BA, Dumoulin SO, Brewer AA. 2007. Visual field maps in human cortex. Neuron. 56:366–383.
Watson JD, Myers R, Frackowiak RS, Hajnal JV, Woods RP, Mazziotta JC, Shipp S, Zeki S. 1993. Area V5 of the human brain: Evidence from a combined study using positron emission tomography and magnetic resonance imaging. Cereb Cortex. 3:79–94.
Weigelt S, Kourtzi Z, Kohler A, Singer W, Muckli L. 2007. The cortical representation of objects rotating in depth. J Neurosci. 27:3864–3874.
Weigelt S, Muckli L, Kohler A. 2008. Functional magnetic resonance adaptation in visual neuroscience. Rev Neurosci. 19:363–380.
Wenderoth P, Wiese M. 2008. Retinotopic encoding of the direction aftereffect. Vision Res. 48:1949–1954.
Xu Y, Turk-Brown NB, Chun MM. 2007. Dissociating task performance from fMRI repetition attenuation in ventral visual cortex. J Neurosci. 27:5981–5985.
Yi DJ, Chun MM. 2005. Attentional modulation of learning-related repetition attenuation effects in human parahippocampal cortex. J Neurosci. 25:3593–3600.
Yi DJ, Kelley TA, Marois R, Chun MM. 2006. Attentional modulation of repetition attenuation is anatomically dissociable for scenes and faces. Brain Res. 1080:53–62.
Yoshor D, Bosking WH, Ghose GM, Maunsell JH. 2007. Receptive fields in human visual cortex mapped with surface electrodes. Cereb Cortex. 17:2293–2302.
Zeki S, Watson JD, Lueck CJ, Friston KJ, Kennard C, Frackowiak RS. 1991. A direct demonstration of functional specialization in human visual cortex. J Neurosci. 11:641–649.